The Tesla Test Facility FEL: Its present status and future as a user facility

Ph. Piot, on the behalf of the TTF-FEL team [1]

Deutsches Elektronen-Synchrotron (DESY), D-22603 Hamburg, Germany

Abstract

The Tesla test facility (TTF), an experimental facility dedicated to the testing of components related to the TESLA linear collider project, has driven a free-electron laser (FEL) since February 2000. The FEL-facility, in its first phase, has served as a proof-of-principle for the self-amplified spontaneous emission (SASE) principle. It has produced FEL-light in the vacuum ultraviolet range (down to ~80 nm), and a series of experiments to study the FEL underlying physics along with two user experiments were conducted.

The TTF-FEL program will soon enter its second phase: it will be upgraded to a user facility capable of reaching the soft X-rays regime (down to 6 nm).

In this paper we review the achievements of TTF-FEL and discuss the challenges and prospects associated to its upgrade to a user facility.

[1] V. Ayvazyan, N. Baboi, I. Bohnet, R. Brinkmann, M. Castellano, P. Castro, L. Catani, S. Choroba, A. Cianchi, M. Dohlus, H.T. Edwards, B. Faatz, A.A. Fateev, J. Feldhaus, K. Flöttmann, A. Gamp, T. Garvey, H. Genz, Ch. Gerth, V. Gretchko, B.Grigoryan, U. Hahn, C. Hessler, K. Honkavaara, M. Hüning, R. Ischebeck, M. Jablonka, T. Kamps, M. Körfer, M. Krassilnikov, J. Krzywinski, M. Liepe, A. Liero, T. Limberg, H. Loos, M. Luong, C. Magne, J. Menzel, P. Michelato, M. Minty, U.-C. Müller, D. Nölle, A. Novokhatski, C. Pagani, F. Peters, J. Pflüger, Ph. Piot, L. Plucinski, K. Rehlich, I. Reyzl, A. Richter, J. Rossbach, E.L. Saldin, W. Sandner, H. Schlarb, G. Schmidt, P. Schmüser, J.R. Schneider, E.A. Schneidmiller, H.-J. Schreiber, S. Schreiber, D. Sertore, S. Setzer, S. Simrock, R. Sobierajski, B. Sonntag, B. Steeg, F. Stephan, K.P. Sytchev, K. Tiedtke, M. Tonutti, R. Treusch, D. Trines, D. Türke, V. Verzilov, R. Wanzenberg, T. Weiland, H. Weise, M. Wendt, T. Wilhein, I. Will, S. Wolff, K. Wittenburg, M.V. Yurkov, K. Zapfe

Presented at SR-2002 July 15-19, Novosibirsk, Russia *13 September 2002*

1 Introduction

In an free-electron laser (FEL), the magnetic field of the undulator magnet causes the electrons to oscillate transversely and at the resonant wavelength [1]:

$$\lambda_{ph} = \frac{\lambda_w}{2\gamma^2}\left(1 + \frac{K^2}{2}\right), \tag{1}$$

where λ_w is the undulator period, K the undulator parameter (that depends upon the peak magnetic field), and γ the Lorentz factor. These waves eventually bunch the electron into micro-bunch on a scale of λ_{ph}. This induced micro-bunching causes electrons within the micro-bunches to radiate coherently at the resonant wavelength. In the oscillator configuration, the laser light reflects back and forth between mirrors, gaining strength on each pass. At ultra-short wavelength, less than 100 nm, mirrors are not available. In such a case and provided the electron bunch has a high phase space density, the FEL instability develops in a single pass through the undulator [2,3]. In this "high gain mode" the radiation power growths exponentially with the position z along the undulator:

$$P(z) = P_o \exp\left(\frac{z}{L_g}\right), \tag{2}$$

where P_o is the power associated to the "seed" radiation and L_g the gain length. In the process referred to as self-amplified stimulated emission (SASE), there is no seeding radiation. Instead the spontaneous radiation generated in the first part of the undulator is used as an input signal. After a sufficient number of gain length (typically $\sim 20L_g$) the electrons run out of resonance and the power reaches its saturation level.

2 Experimental results from TTF-FEL 1

2.1 experimental set-up

The experimental results presented herafter were obtained at TTF-FEL 1 (Fig. 1) [4]. The injector is based on a photo-emission rf-gun electron source [5]. A UV-laser impinges a Cesium Telluride photo-cathode mounted on the back plate of a 1-1/2 cell radio-frequency (rf) cavity operating at $f = 1.3$ GHz. The photo-emitted electrons are accelerated up to approximately 4 MeV (an electric field of 37 MV/m is applied on the photo-cathode). The UV laser pulse has a Gaussian time distribution with a rms length of 7 ps. Under nominal operating conditions of TTF-FEL 1, the laser repetition rate is operated up to 2.25 MHz and the rf-field in the cavity is sustained for up to 800 μsec at a frequency of 1 Hz. Thus the source is able to provide macropulses of 800 μsec with 1200 bunches. The charge per bunch is approximately 4 nC. The rf-gun is followed by a 9-cell TESLA-type superconducting cavity, the booster, that accelerates the beam to 16 MeV. Downstream, two TESLA accelerating modules bring the beam energy up to 300 MeV. An accelerating module consists of eight 9-cell superconducting standing wave rf cavities operating on the π-mode. A magnetic bunch compression located between the two accelerating modules is used to shorten the electron bunch. In this scheme, a (linear) time-energy correlation is impressed on the bunch by properly tuning the first accelerating module. The magnetic bunch compressor, a four bends achromatic chicane, introduces an energy dependent path length. Thus by introducing a time-energy correlation such that the bunch head has a lower energy than the tail, the bunch can be shortened. In practice the compression might be limited by nonlinear effects as in TTF-FEL 1 (see Fig. 2): the incoming bunch being too long, the time-energy correlation accumulates a cos-like distortion as the bunch passes through the first accelerating module. Such a distortion impacts the compression by giving rise, downstream of the

bunch compressor, to highly non-Gaussian charge density with local charge concentration [6]. After the second module, a set of quadrupoles provides the required optical matching of the electron beam parameters into the undulator. A transverse collimation system insures the beam cannot be lost within the undulator [7].

The undulator is a permanent magnet device [8] with a 12 mm gap and an undulator parameter of $K = 1.17$. Permanent quadrupole magnets, arranged as a FODO structure, are superimposed on the periodic undulator field in order to focus the electron beam along the undulator. The undulator system consists of three segments, each 4.5 m long. Within the segments, the vacuum chamber incorporates beam position monitors and dipole magnets that provide control on the beam trajectory.

Downstream, once the electron and photon beams have been separated, the beamline is equipped with a suite of photon diagnostics that allow the measurement of radiation intensity, spectrum, and transverse distribution[9].

2.2 SASE free-electron laser physics

2.2.1 exponential growth and saturation

The average energy of the radiation measured as a function of the active undulator length is compared in Figure 3 with numerical simulations performed with the program FAST [10]. The active undulator length is defined as the length where the electron and photon beams overlap. Such an overlap can be altered by using dipoles to steer the electron beam away from the undulator axis. Figure 3 clearly exhibits the exponential growth rate of the radiation energy as expected from Eqn (2). Also observable is the saturation regime for $z > 12$ m. From the Figure we concluded the FEL gain to be about 10^7 [11].

2.2.2 statistical properties

Shot noise in the beam cause fluctuation of the beam density. As a result in the linear regime the radiation energy is expected to fluctuate according to a Gamma distribution characterized by the single parameter $M = \langle E \rangle^2 / \sigma_E^2$ where $\langle E \rangle$ and σ_E are respectively the mean and variance energy of the probability distribution. The parameter M indeed corresponds to the number of optical longitudinal modes [12]. The measured pulse energy probability distributions by accumulating data over 10 mins time laps are presented in Figure. 4 for both a "long" and "short" electron bunch settings (these two settings simply corresponds to different tuning of the bunch compressor). The observed distribution is in good agreement with the Gamma distribution. As expected the "short" electron pulse setting has higher fluctuations (i.e. have a smaller number of modes M) than the "long" one.

2.2.3 spectrum

Spectral measurements of the radiation provide an indirect estimate of the time structure of the SASE radiation: given the spectrum FWHM width $\delta\omega$, the time duration of the SASE pulse is $\tau_{rad} \sim 2\pi/\delta\omega$. In Figure 4, the measured spectra for the two aforementioned "short" and "long" electron pulses settings are compared. The estimated time duration is $\tau_{rad} \simeq 50$ fs and $\simeq 100$ fs respectively.

2.2.4 transverse coherence

As the beam propagates along the undulator, the SASE field amplitude is dominated by the fundamental mode (since it is the one with the largest growth rate). The fact that the radiation is dominated by a single mode means it is completely coherent transversely. The diffraction pattern observed on a Ce:Yag screen located 3 m downstream of set of two parallel slits is presented

in Fig. 5. The remarkable high fringe visibility confirms the high degree of transverse coherence.

3 Upgrade to a soft X-ray user-facility: TTF-FEL 2

To reach lower wavelength down to 6 nm, the TTF-FEL will be upgraded [13]. The linac will incorporate three additional accelerating modules to boost the energy to 1 GeV, the injector and the bunch compression scheme will be re-built (see Fig. 1) to generate the required normalized transverse emittance $\varepsilon < 2$ mm-mrad and peak current $I_{peak} > 2.5$ kA [14,15].

The injector will incorporate a new cylindrically symmetric rf-gun to avoid transverse emittance growth induced by the rf-field asymmetry introduce by the side rf-coupler in the TTF-FEL 1 rf-gun. The photocathode drive-laser will be upgraded to be capable of generating plateau-like time distribution since this latter type of distribution is known to reduce nonlinear space charge force and its associated emittance growth. The electrons generated from the rf-gun will directly be injected in an accelerating module that accelerates the beam up to 140 MeV. A third harmonic ($f = 3.9$ GHz) rf-structure will be used to correct for the nonlinear distortions of the longitudinal phase space thereby avoiding the typical fold over of the longitudinal phase space as observed at TTF-FEL 1 (as pictured in Fig. 2).

To compress the bunch down to the proper bunch length (i.e. to achieve a peak current of 2.5 kA) while negotiating space-charge induced beam degradation, TTF-FEL 2 incorporates a two stages magnetic compression scheme. The first magnetic compressor is located downstream of the third harmonic cavity, in the injector area. It shortens the rms bunch length from 2.2 to $\sim$ 0.4 mm. The chicane is similar to the 4-bend chicane designed for TTF-FEL 1. The second stage compression occurs downstream of the third accelerating module

at 440 MeV. The chicane chosen is a wiggler-type chicane optimized to have a minimum emittance dilution due to coherent synchrotron radiation [16]. The final rms bunch length is approximately 50 μm.

The whole TTF-FEL 2 accelerator has been extensively simulated taking into account realistic electron beam distributions generated by computer programs that account for the space charge effects at low energy, the bunch self-interaction via coherent synchrotron radiation in bunch compressors, and the impacts of the geometric wake fields in the TESLA-cavities. An example of the obtained longitudinal distribution at the undulator entrance is presented in Figure 6 along with the expected performance of the FEL. The FEL simulation were performed by directly simulated electron distribution in the program FAST. This example of start-to-end simulation shows that the bunch provided by TTF-FEL 2 driver-accelerator should enable the operation of the SASE FEL in the saturation regime with peak power exceeding 5 GW.

4 Outlook

The TTF-FEL 1 has demonstrated the feasibility of radiation source in the VUV regime using the SASE principle. The achieved peak brilliance of 2×10^{28} photons/ (s.mrad^2.mm^2.0.1% bandwidth) exceeds the other sources by several orders of magnitude. Ultra short radiation pulses with peak power of 1 GW have been generated. Since the TTF-FEL is driven by a superconducting accelerator, it has also the potential to reach high average brilliance (comparable to storage ring-based light sources). TTF-FEL 1 has generated radiation pulses with tunable wavelength (80 nm$< \lambda_{ph} <$120 nm demonstrated) and pulse length (down to 30 fs achieved). TTF-FEL 1 has demonstrated the maturity of the required technology for the foreseen TESLA X-ray FEL in the Ängstrom regime [17] and will soon be upgraded to a user facility in the soft

X-ray regime.

Electrons:	
beam energy	$220 - 270$ MeV
bunch charge	2.7-3.3 nC
charge in lasing part of bunch	0.1-0.3 nC
duration of radiative part of bunch	50-150 fs
peak current	1.3 ± 0.3 kA
rms normalized emittance	(6 ± 2) mm$-$mrad
Undulator:	
undulator period λ_u	27.3 mm
undulator peak field	0.47 T
average beta-function	1.2 m
magnetic length of undulator	13.5 m
Photons:	
radiation wavelength	80-120 nm
energy in the radiation pulse	$30 - 100$ μJ
FWHM radiation pulse duration	$50 - 200$ fs
radiation peak power level	1 GW
spectral width (FWHM)	1%
rad. spot size at undulator exit (FWHM)	250 μm
radiation angular divergence (FWHM)	260 μrad

Table 1
Summary of the main parameters achieved at TTF-FEL 1.

Fig. 1. Overview of the TTF-FEL programs: TTF-FEL 1 **(a)** and TTF-FEL 2 **(b)**. BC: bunch compressor, ACC: accelerating module.

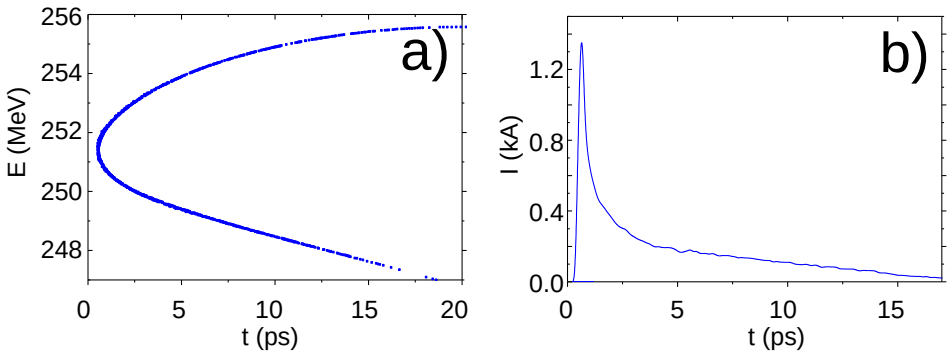

Fig. 2. Longitudinal phase space **(a)** and corresponding current distribution **(b)** for the electron bunch downstream of the magnetic bunch compressor ($t > 0$ correspond to the bunch tail).

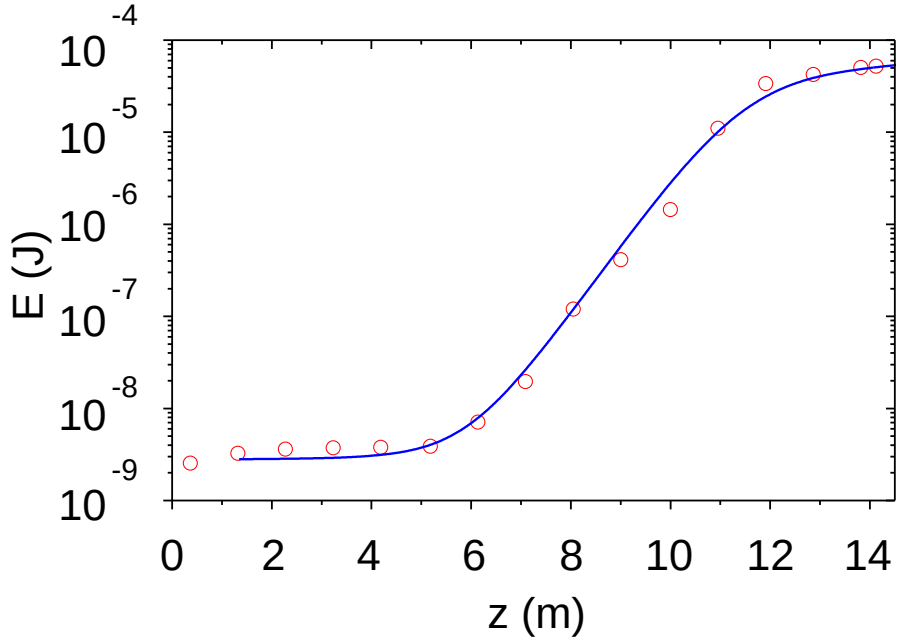

Fig. 3. Average energy in the radiation pulse as a function of the active undulator length. Circles: experimental results. Solid curve: numerical simulations with the code FAST [10], using parameters of Table 1.

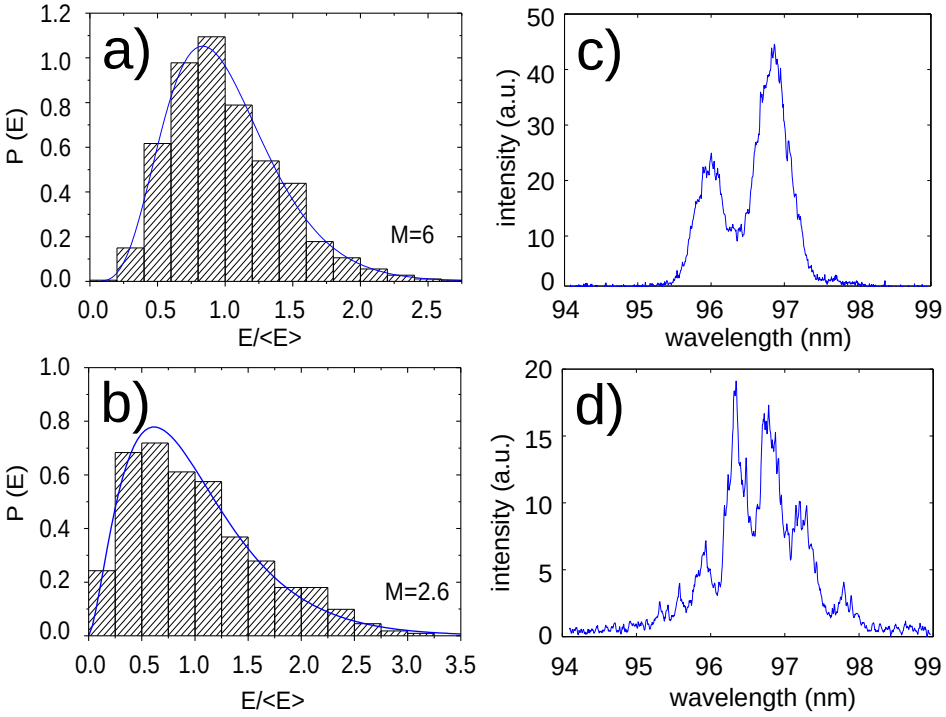

Fig. 4. Statistical fluctuation of the SASE energy for "short" **(a)** and "long" **(b)** bunch length settings and corresponding radiation spectrum for the same "short" **(c)** and "long" **(d)** settings.

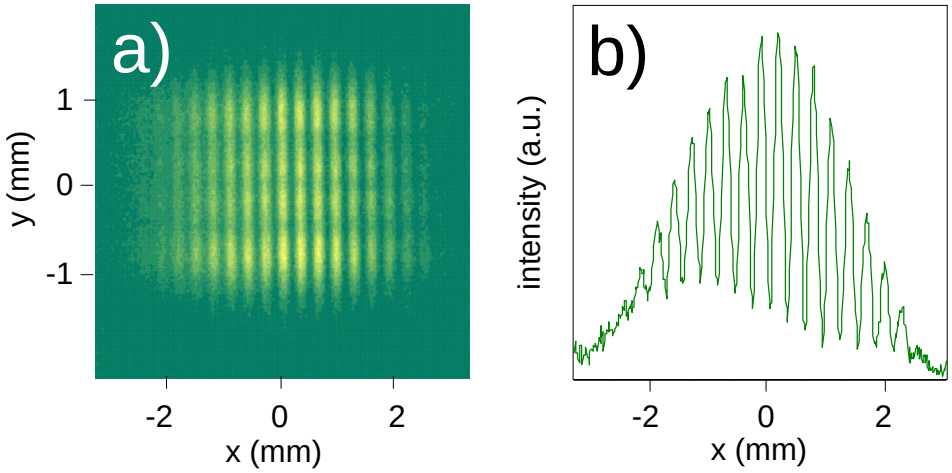

Fig. 5. Diffraction patterns of a double slit seperated by 1 mm. Image on the Ce:YaG screen **(a)** and corresponding horizontal projection **(b)**.

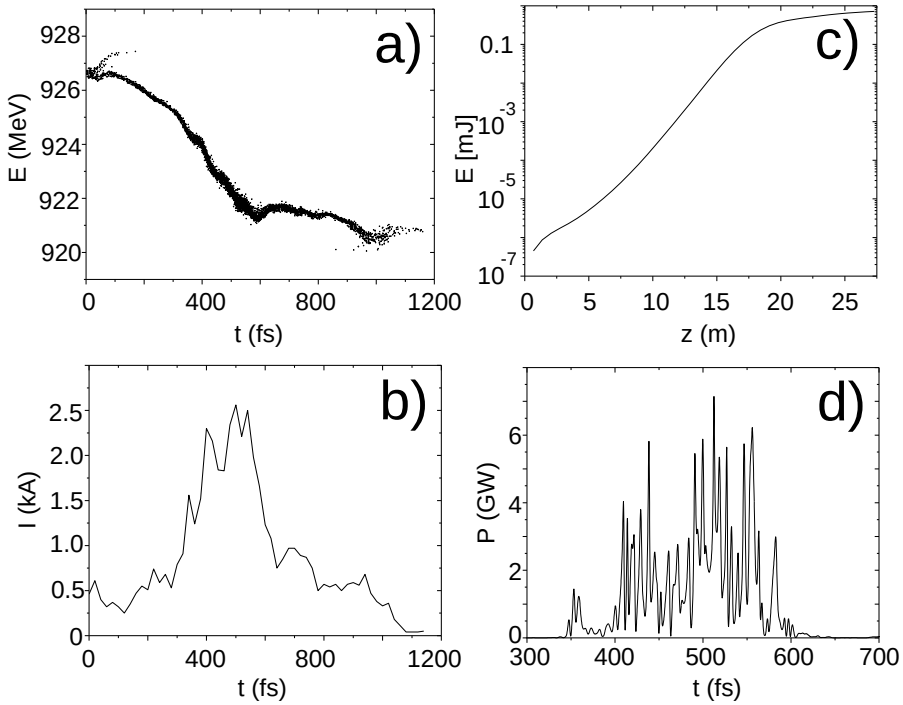

Fig. 6. Nominal operation settings for the TTF-FEL 2. Longitudinal phase space **(a)** and current distribution **(b)** for the electron bunch. Energy of the radiation along the undulator **(c)** and power along the SASE pulse at the undulator exit **(d)**.

References

[1] Madey J.M.J, *J. Appl. Phys.* **42**, 1906 (1971)

[2] Kondratenko A. M., Saldin E. L., *Part. Acc.* **10**, 207 (1980)

[3] Bonifacio R., Pelligrini C., Narducci L. M., *Opt. Comm.* **50**, 373 (1984)

[4] Andruszkow J., et al, *Phys. Rev. Lett.* **85**, 3818 (2002)

[5] Schreiber S., et al, "Improved operation of the TTF photoinjector for FEL operation" in proceedings of EPAC 2002 (in press)

[6] Limberg T., Piot Ph., Schneidmiller E.A., Nucl. Instr. and Meth. **A475**, 353 (2001).

[7] Schlarb H., "Design and performance of the TTF collimation system" in proceedings of EPAC 2002 (in press)

[8] J. Pflüger, Nucl. Instr. and Meth. **A445**, 366 (2000)

[9] R. Treusch, et al, Nucl. Instr. and Meth. **A445**, 456 (2000)

[10] E.L. Saldin, E.A. Schneidmiller, M.V. Yurkov, Nucl. Instr. and Meth. **A429**, 233 (1999).

[11] Ayvazian V., et al, *Phys. Rev. Lett.* **88**, 104802 (2002)

[12] E.L. Saldin, E.A. Schneidmiller, M.V. Yurkov, Opt. Commun. **148**, 383 (1998).

[13] *SASE FEL at the TESLA Facility - phase 2*, TESLA-FEL report 02-01, DESY (2002)

[14] Flöttmann K. and Piot Ph., TESLA-FEL report 02-04, DESY (2002)

[15] Limberg T. Piot Ph. and Stulle F., "Design and performance simulation of the TTF-FEL II bunch compression" in proceedings of EPAC 2002 (in press)

[16] Derbenev Ya., et al, TESLA-FEL report 95-05, DESY (1995)

[17] *TESLA Technical design report* DESY 2001-001 (2001)